

See discussions, stats, and author profiles for this publication at: <https://www.researchgate.net/publication/231640042>

Control Growth of One-Dimensional Nanostructures of Organic Materials

ARTICLE *in* THE JOURNAL OF PHYSICAL CHEMISTRY B · MAY 2004

Impact Factor: 3.3 · DOI: 10.1021/jp049455r

CITATIONS

23

READS

16

9 AUTHORS, INCLUDING:



Huibiao Liu

Chinese Academy of Sciences

236 PUBLICATIONS 6,225 CITATIONS

SEE PROFILE



Shengqiang Xiao

Wuhan University of Technology

49 PUBLICATIONS 1,507 CITATIONS

SEE PROFILE



Lei Jiang

Yunnan Agricultural University

139 PUBLICATIONS 4,838 CITATIONS

SEE PROFILE



Dapeng Yu

Peking University

591 PUBLICATIONS 16,097 CITATIONS

SEE PROFILE

Control Growth of One-Dimensional Nanostructures of Organic Materials

Huibiao Liu,[†] Yuliang Li,^{*,†} Shengqiang Xiao,[†] Hongmei Li,[†] Lei Jiang,[†] Daoben Zhu,^{*,†} Bin Xiang,[‡] Yaofeng Chen,[‡] and Dapeng Yu[‡]

Center for Molecular Sciences, Institute of Chemistry, Chinese Academy of Sciences, Beijing 100080, and Department of Physics, Peking University, Beijing 100871, People's Republic of China

Received: February 6, 2004; In Final Form: March 16, 2004

We have developed a useful and experimentally easy way using organic molecule AQ (9,10-anthraquinone) powders under controlled conditions in the presence of a catalyst to directly fabricate AQ nanotube junctions, nanotubes, and nanorods. The approach should have an outstanding potential in providing customized nanotubes and nanotube junctions for a broad range of applications in nanoscience.

Introduction

The development of a convenient preparation of nanostructures and systematic control over their shape and properties are the main objectives of materials science. Particularly, control over shape and hence over dimensionality is of great interest with regard to potential applications of such materials as electronic, photonic, and optoelectronic devices.^{1–6} To generate junctions between two or more nanotubes is a key for achieving the functionality of these nanotubes as building blocks in potential devices. A wide range of materials, including semiconductors,⁷ oxides,⁸ metals,⁹ polymers,¹⁰ and especially carbon nanotubes,^{11–14} have been made into various kinds of junctions. However, the challenge of synthetically controlling the shape, especially the shape of organic molecule aggregates, has not been paid attention. Recently, there has been more attention attracted to the fabrication of 1D organic nanoscale materials due to their properties being completely different from those of inorganic and polymeric materials. There are some preparation methods that have been reported for preparing organic 1D nanostructure materials, such as mask shadowing vapor deposition¹⁵ and self-assembly on flat substrates (KCl crystals, HOPG).¹⁶ We have been developing new methods for controlling organic nanomaterial growth for fabricating low dimensions of nanotubes, nanotube junctions, and nanowires.^{17,18} Herein, we report a simple method through thermal evaporation of 9,10-anthraquinone (AQ) powders in the presence of zinc catalyst to produce nanotubes, nanotube junctions, and nanorods.

Experimental Section

Growing nanotubes, nanotube junctions, and nanorods of AQ is achieved by thermal evaporation of AQ powders under controlled conditions in the presence of zinc catalyst. All chemical reagents were purchased from Beijing Chemical Reagents Corp. Copper wafers (50 mm × 10 mm × 0.6 mm) are used after being cleaned in an ultrasonic bath of acetone for 20 min, 0.1 M HCl for 15 min, deionized water for 10 min, and ethanol for 10 min. The mixture of AQ (mp 286 °C, bp 379–381 °C) and zinc powders was loaded into a ceramic boat and then placed at the center of a quartz tube (800 mm in length and 35 mm in inner diameter) that was inserted into a horizontal

tube furnace. The copper wafer was placed at the downstream end of the quartz tube and was 15 cm away from the ceramic boat. The reaction temperature and time were controlled. In our experiments, except for the evaporation temperature, which was determined on the basis of the melting point and boiling point of organic materials, the following parameters were kept constant: evaporation time, 2 h; argon gas flow rate. The furnace temperature was first increased to the appropriate temperature and then kept at that temperature for 2 h. Finally, the temperature was allowed to descend to room temperature. In the process, the argon gas flow rate was kept constant at an appropriate value. During evaporation, the products were deposited onto a copper wafer placed at the downstream end of the quartz tube. The as-deposited products were characterized and analyzed by scanning electron microscopy (SEM), transmission electron microscopy (TEM), infrared (IR) spectroscopy, and EI mass spectrometry (VG-ZAB-HS EI). SEM images were obtained with a JEOL JSM 6700F and DB-235 FIB field emission scanning electron microscope. TEM images were taken with a Tecnai F30 microscope operating at 200 keV. The X-ray diffraction (XRD) patterns were recorded with a Japan Rigaku D/max-2500 rotation anode X-ray diffractometer equipped with graphite-monochromatized Cu K α radiation ($\lambda = 1.541\ 78\ \text{\AA}$), employing a scanning rate of 0.05 deg s⁻¹ in the 2 θ range from 10° to 90°.

Results and Discussion

Under argon gas with a flow rate of 100 standard cm³/min, thermal evaporation of AQ powders under controlled conditions in the presence of zinc catalyst at 340 °C for 2 h resulted in products that formed on the surface of the copper wafer. The as-synthesized products can be obtained for several morphologies. SEM images (Figure 1) reveal that the products consist of a large quantity of nanotube junctions and nanotubes. Figure 1A shows that the geometrical shapes of AQ nanotube junctions are mono-cross-shaped and poly-cross-shaped. We can observe that there is perfect symmetry between two arms in every nanotube junction. Each nanotube junction has a uniform length, diameter, and side tubes. The typical lengths of the six-cross nanotube junctions are in the range of 2–10 μm , while their diameters are in the range of 400 nm to 2 μm (Figure 1B). Figure 1C shows that the lengths and the diameters of a typical polycross with an eight-arm nanotube junction are about 5 and

[†] Chinese Academy of Sciences.

[‡] Peking University.

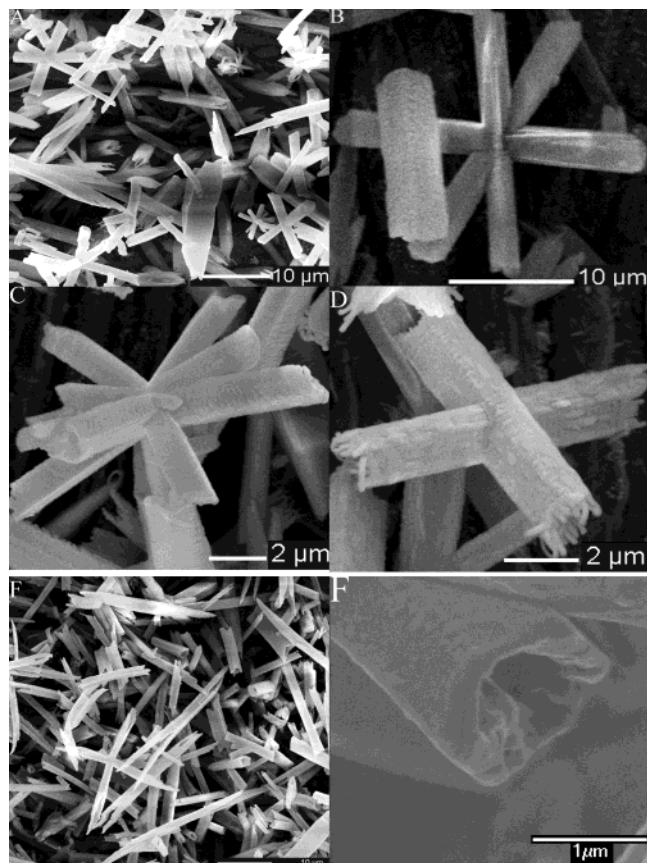


Figure 1. SEM images of the as-synthesized AQ junction and nanotubes: (A) AQ nanotube junctions and AQ nanotubes, (B) a single typical polycross with a six-arm nanotube junction, (C) a typical polycross with an eight-arm nanotube junction, (D) a perfectly symmetric cross-shaped nanotube junction, (E) low-magnification SEM image of AQ nanotubes, (F) a typical AQ nanotube.

1–2 μm , respectively. To cross-shape nanotube junctions, their lengths and diameters must be in the range of 1–5 μm and 500–800 nm, respectively. The polycross with an eight-arm nanotube junction is uniform with regard to their lengths and diameters. The lengths and diameters of the AQ nanotubes are from several micrometers to several tens of micrometers and from several hundred nanometers to several micrometers, respectively, which are similar to those of the nanotube junctions

(Figure 1E). Figure 1F shows that the outer diameter of a typical single AQ nanotube is about 1.2 μm , while the inner diameter is about 850 nm.

For TEM analysis of the nanotubes and nanotube junctions of AQ molecules obtained from as-synthesized products, the image in Figure 2A shows a typical individual polycross with an eight-arm nanotube junction. The diameter of every arm is in the range of about 400–600 nm, and the thickness of the wall is in the range of about 200–300 nm. Figure 2B depicts that the diameter of the AQ nanotube is about 450 nm and the thickness of the wall is about 380 nm. The surfaces of all nanotubes and nanotube junctions are not smooth. The FT-IR spectra (Figure 3A) of nanotubes and nanotube junctions show typical AQ molecular absorption bands at 1677, 1591, 1284, 937, and 694 cm^{-1} . The result indicates that the nanotubes and nanotube junctions still remain the structural characteristic of AQ molecules. The XRD pattern (Figure 4A) shows that the products are crystallized well. It is noted that the diffraction peak of (111) was stronger than expected. This unusual diffraction peak of (111) indicates a preferential orientation along the *c* axis and a quasi-one-dimensional shape, which is consistent with the characteristic results of TEM and SEM.

Under the same conditions, decreasing the evaporation temperature to 280 $^{\circ}\text{C}$ with an argon gas flow rate of 60 standard cm^3/min , the AQ nanorods formed on the surface of the copper wafer. The SEM images show that the morphology found in the as-grown sample is the rod shape (Figure 5A,B). Figure 5A shows that the AQ nanorods are apt to orient in arrays on the surface of the copper wafer. The length of the AQ nanorods is from several hundred nanometers to several micrometers, while the diameter is in the range of 110–210 nm (Figure 5B). TEM images (Figure 5C) show that the lengths of the AQ nanorods are 500 nm to 1.6 μm , and the diameters are 60–270 nm. The diameters of most nanorods are 100 nm, which is consistent with the results of SEM. The characteristic absorptions at 1677, 1590, 1285, 939, and 696 cm^{-1} in the FT-IR spectrum (Figure 3B) of nanorods indicate that the nanorods still remain the structural characteristic of AQ molecules. The XRD pattern (Figure 4B) shows that the products are similar to the AQ nanotubes and nanotube junctions, for which the stronger diffraction peak of (111) indicates a preferential orientation along the *c* axis and a quasi-one-dimensional shape.

No metal droplet is found at the end of nanotubes, nanotube junctions, and nanorods. It has been suggested that the 1D

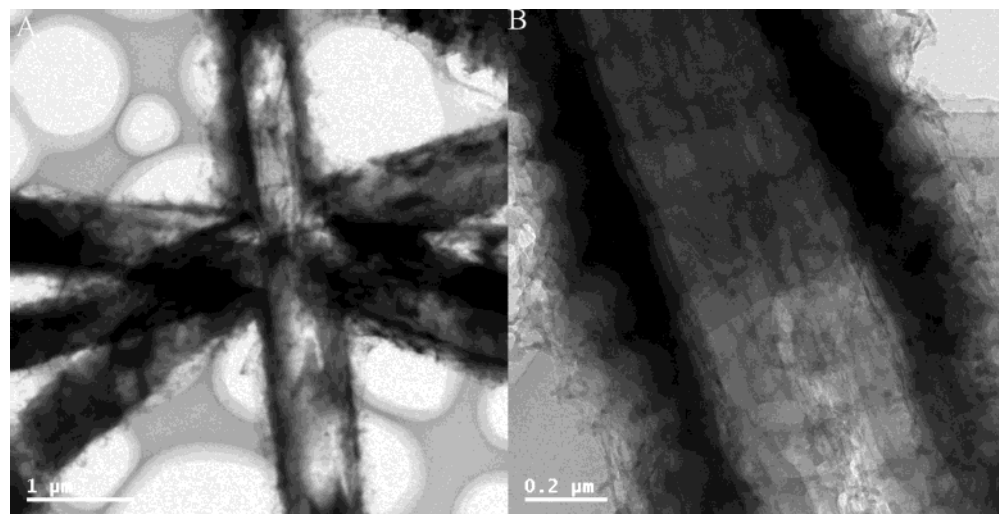


Figure 2. TEM images of the as-synthesized AQ junction and nanotubes: (A) an individual polycross with an eight-arm AQ nanotube junction, (B) a single typical AQ nanotube.

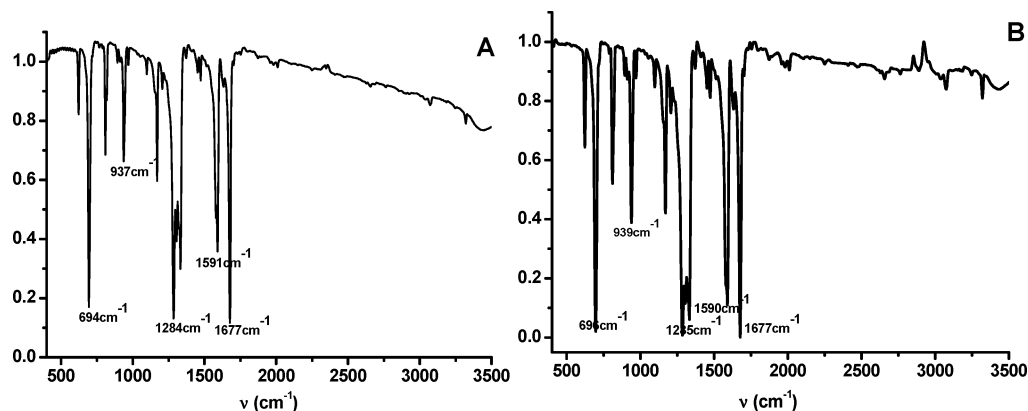


Figure 3. FT-IR spectra (KBr): (A) AQ nanotubes and nanotube junctions, (B) AQ nanorods.

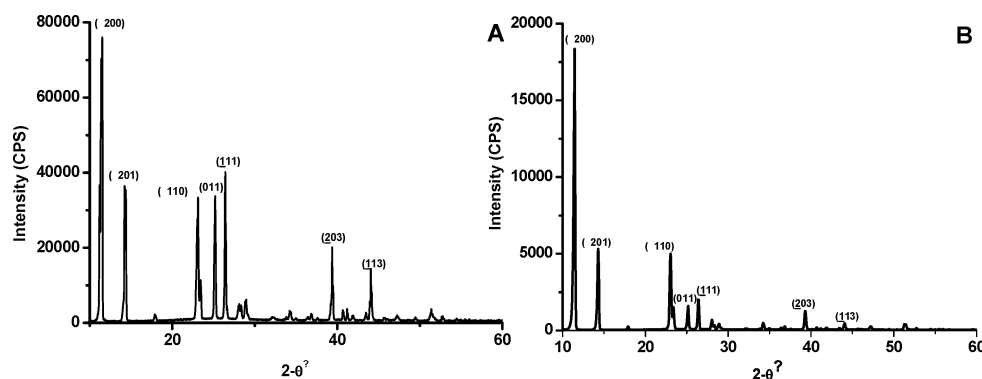


Figure 4. XRD patterns: (A) AQ nanotubes and nanotube junctions, (B) AQ nanorods.

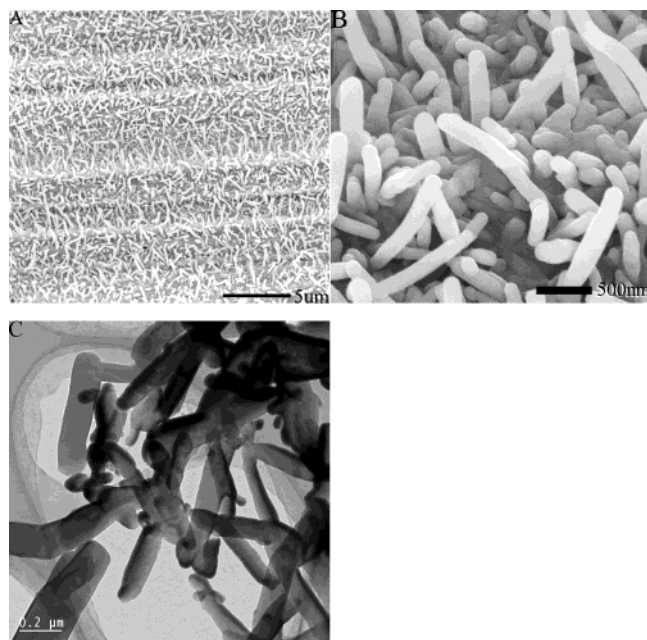


Figure 5. (A) Low-magnification SEM image of AQ nanorods. (B) High-magnification SEM image of AQ nanorods. (C) TEM image of AQ nanorods.

nanomaterials may not be dominated by the vapor–liquid–solid (VLS) process¹⁹ proposed for the nanotubes grown by a catalytic-assisted technique, in which a metal particle is located at the growth front of the wire and acts as the catalytic active site. Because the zinc powders have not been evaporated or melted at the synthesis temperature, it is likely that the growth is governed by a vapor–solid process.²⁰ In the synthesis process, the AQ vapors are carried by the inert gas stream to the downstream end where the temperature is lower than that of

the center of the furnace, and the organic vapors will deposit on the wafer and inner surface of the quartz tube and grow into 1D nanostructures. The wafer is a very important factor for growing 1D nanostructures. If we replaced a copper wafer with a silicon wafer, we only obtained an AT needlelike structure (Figure S1A in the Supporting Information), whose diameter is in the range of 3–8 μm . This may be due to the formation of a surface-supported supramolecular structure whose size and aggregation shape are rationally controlled by the interactions between individual oxygen atoms on AQ molecules and copper atoms on the surface of the copper wafer, as well as interactions of hydrogen bonds between the oxygen atoms on the AQ molecule and hydrogen atoms on the aromatic ring of another AQ molecule,²¹ which suggests that the self-assembly of 1D nanostructures is rather uniform and is also in good arrangement. If we used anthracene (AN), which does not contain oxygen atoms, to replace AQ molecules, only the flake-shaped product was deposited on the copper wafer (Figure S1B). In the absence of zinc catalyst in the reaction system, many irregular morphologies of AQ nanostructures formed (Figure S1C). If Mg or Fe powders were used instead of zinc powder, the uniform nanostructures of AQ as mentioned above were not obtained. It is possible that the vapor–solid (VS) process and self-assembly by hydrogen bonds between the oxygen atoms on AQ molecules and hydrogen atoms on another AQ molecule are the main factors for the growth mechanism of 1D nanostructures on the surfaces of the copper wafer. We suggest that the characteristic intermolecular interaction between the Cu–O face and hydrogen atoms of the aromatic ring of the AQ molecule are exploited to influence the supramolecular aggregation. The morphology and shape of the products are also found to strongly depend on the reaction temperature. The synthesis temperature is adjacent to the boiling point of AQ; we observed that only the typical yellow needle crystals are formed.

Conclusion

We have successfully prepared organic molecular nanotubes, nanotube junctions, and nanorods from organic compound powders through the combination of thermal evaporation and the self-assembly technique. The efficient method enlarges the family of nanotubes, junctions, and nanorods significantly from inorganic and polymer to organic small molecules. This approach is expected to form a new general route for the controlled morphology—synthesis of organic molecular materials in restricted dimensions, with controlled size and shape. The solid-state physical properties of these organic nanostructures are of great interest. As demonstrated above, the approach should have an outstanding potential in providing customized nanotubes, nanotube junctions, and nanorods for a broad range of applications in nanoscience.

Acknowledgment. We are most grateful to Professor Sishen Xie for his insights and encouragement. This work was supported by the Major State Basic Research Development Program and the National Nature Science Foundation of China (Grants 20151002, 50372070, and 90101025).

Supporting Information Available: SEM images of AQ deposited on a silicon wafer, AN deposited on a copper wafer, and AQ deposited on a copper wafer without the use of a zinc catalyst (PDF). This material is available free of charge via the Internet at <http://pubs.acs.org>.

References and Notes

- (1) (a) Duan, X. F.; Huang, Y.; Wang, J. F.; Lieber, C. M. *Nature* **2001**, *409*, 66. (b) Cui, Y.; Lieber, C. M. *Science* **2001**, *291*, 851.
- (2) (a) Messer, B.; Song, J. H.; Yang, P. *J. Am. Chem. Soc.* **2000**, *122*, 10232. (b) McEuen, P. L. *Nature* **1998**, *393*, 15.
- (3) (a) Peng, X. G.; Manna, L.; Yang, W. D.; Wickham, J.; Scher, E.; Kadavanich, A.; Alivisatos, A. P. *Nature* **2000**, *404*, 559. (b) Schlamp, M. C.; Peng, X. G.; Alivisatos, A. P. *J. Appl. Phys.* **1997**, *82*, 5837.
- (4) (a) Huang, M. H.; Mao, S.; Feick, H.; Yan, H.; Wu, Y.; Kind, H.; Weber, E.; Russo, R.; Yang, P. *Science* **2001**, *292*, 1897. (b) Pan, Z. W.; Dai, Z. R.; Wang, Z. L. *Science* **2001**, *291*, 1947.
- (5) Chan, E. M.; Mathies, R. A.; Alivisatos, A. P. *Nano Lett.* **2003**, *3*, 199.
- (6) Liu, H.; Li, Y.; Jiang, L.; Luo, H.; Xiao, S.; Fang, H.; Li, H.; Zhu, D.; Yu, D.; Xu, J.; Xiang, B. *J. Am. Chem. Soc.* **2002**, *124*, 13370.
- (7) Hu, J.; Ouyang, M.; Yang, P.; Lieber, C. M. *Nature* **1999**, *399*, 48.
- (8) Wang, Z.; Pan, Z. *Adv. Mater.* **2002**, *14*, 1029.
- (9) (a) Mbindyo, J. K. N.; Mallouk, T. E.; Mattzela, J. B.; Kratochvilova, I.; Razavi, B.; Jackson, T. N.; Mayer, T. S. *J. Am. Chem. Soc.* **2002**, *124*, 4020. (b) Bumm, L. A.; Arnold, J. J.; Cygan, M. T.; Dunbar, T. D.; Burgin, T. P.; Jones, L.; Allara, D. L.; Tour, J. M.; Weiss, P. S. *Science* **1996**, *271*, 5256. (c) Reed, M. A.; Zhou, C.; Muller, C. J.; Burgin, T. P.; Tour, J. M. *Science* **1997**, *278*, 5336. (d) Fan, F. R. F.; Yang, J. P.; Cai, L. T.; Price, D. W.; Dirk, S. M.; Kosynkin, D. V.; Yao, Y. X.; Rawlett, A. M.; Tour, J. M.; Bard, A. J. *J. Am. Chem. Soc.* **2002**, *124*, 5550. (e) Seminario, J. M.; Zacarias, A. G.; Tour, J. M. *J. Phys. Chem. A* **1999**, *103*, 7883.
- (10) (a) Kovtyukhova, N. I.; Martin, B. R.; Mbindyo, J. K. N.; Smith, P. A.; Razavi, B.; Mayer, T. S.; Mallouk, T. E. *J. Phys. Chem. B* **2001**, *105*, 8762. (b) Cassagneau, T.; Mallouk, T. E.; Fendler, J. H. *J. Am. Chem. Soc.* **1998**, *120*, 7848.
- (11) Li, J.; Papadopoulos, C.; Xu, J. *Nature* **1999**, *420*, 253.
- (12) Kouwenhoven, L. *Science* **1997**, *275*, 1896.
- (13) Zhang, Y.; Ichihashi, T.; Landree, E.; Nihey, F.; Iijima, S. *Science* **1999**, *285*, 1719.
- (14) Satishkumar, B. C.; Thomas, P. J.; Govindaraj, A.; Rao, C. N. R. *Appl. Phys. Lett.* **2000**, *77*, 2530.
- (15) (a) Yanagi, H.; Morikawa, T. *Appl. Phys. Lett.* **1999**, *75*, 187. (b) Balzer, F.; Bordo, V. G.; Simonsen, A. C.; Rubahn, H.-G. *Phys. Rev. B* **2003**, *67*, 115408.
- (16) Loi, S.; Wiesler, U.-M.; Butt, H.-J.; Müllen, K. *Chem. Commun.* **2000**, 1169. (b) Massey, J.; Power, K. N.; Manners, I.; Winnik, M. A. *J. Am. Chem. Soc.* **1998**, *120*, 9533. (c) Chechik, V.; Crooks, R. M. *Langmuir* **1999**, *15*, 6364. (d) Krisel, J. W.; Tilley, T. D. *Chem. Mater.* **1999**, *11*, 1190.
- (17) Liu, H. B.; Li, Y. L.; Jiang, L.; Luo, H. Y.; Xiao, S. Q.; Fang, H. J.; Li, H. M.; Zhu, D. B.; Yu, D. P.; Xu, J.; Xiang, B. *J. Am. Chem. Soc.* **2002**, *124*, 13370.
- (18) Liu, H. B.; Li, Y. L.; Xiao, S. Q.; Gan, H. Y.; Jiu, T. G.; Li, H. M.; Jiang, L.; Zhu, D. B.; Yu, D. P.; Xiang, B.; Chen, Y. F. *J. Am. Chem. Soc.* **2003**, *125*, 10794.
- (19) Wagner, R. S.; Ellis, W. C. *Appl. Phys. Lett.* **1964**, *4*, 89.
- (20) Yang, P. D.; Lieber, C. M. *J. Mater. Res.* **2000**, *12*, 2981.
- (21) Kim, K. S.; Suh, S. B.; Kim, J. C.; Hong, B. H.; Lee, E. C.; Yun, S.; Tarakeshwar, P.; Lee, J. Y.; Kim, Y.; Ihm, H.; Kim, H. G.; Lee, J. W.; Kim, J. K.; Lee, H. M.; Kim, D.; Cui, C.; Youn, S. J.; Chung, H. Y.; Choi, H. S.; Lee, C.-W.; Cho, S. J.; Jeong, S.; Cho, J.-H. *J. Am. Chem. Soc.* **2002**, *124*, 14268.